AIAA JOURNAL
Vol. 45, No. 3, March 2007

Optimization of Geometrically Nonlinear Thin Shells Subject to Displacement and Stability Constraints

Peyman Khosravi,* Ramin Sedaghati,† and Rajamohan Ganesan‡
Concordia University, Montreal, Quebec H3G 1M8, Canada

DOI: 10.2514/1.22714

A methodology is developed for shape optimization of thin plate and shell structures undergoing large deflections subject to displacement and system stability constraints. The optimization method considers shape parameters and overall thickness of the structure as the design variables and aims to minimize the total mass of the structure subject to stability or displacement constraint. Two optimality criteria based on Karush–Kuhn–Tucker conditions are developed for mass minimization problems. Optimality criteria are combined with nonlinear corotational analysis to optimize structures with geometric nonlinearity. The method is applied to plate and shallow shell structures. The efficiency of the developed design optimization methodology is compared with that of the gradient-based method of optimization (sequential quadratic programming).

Nomenclature

$[A^e]$	=	stretching stiffness matrix
A_i	=	area of the ith shell element
$[B^e]$	=	membrane-bending coupling stiffness matrix
$[D^e]$	=	bending stiffness matrix
$\{\boldsymbol{d}\}$	=	element nodal displacement vector in local coordinate system
$[E]$	=	elasticity matrix
$E_\circ$	=	Young's modulus
e_i	=	strain energy of the ith shell element
$\hat{e}_i$	=	strain energy density of the ith shell element
e_{ib}	=	strain energy provided by bending and membrane-bending coupling effects in the ith shell element
F_{cr}	=	limit load of the structure
G	=	shear modulus
h_1, h_2, h_3	=	heights of the spherical shell at different levels
k	=	number of elements affected by the shape design variable x_*
$[k_i]$	=	stiffness matrix of the ith shell element
$\mathcal{L}$	=	Lagrangian function
M	=	total mass
m	=	number of nodal displacement components
N	=	number of the elements
N_e	=	total number of elements affected by all shape design variables
n	=	number of layers in laminated composite shell
R	=	radius of the spherical shell
$\{\boldsymbol{R}\}$	=	vector of the externally applied loads
r	=	step-size parameter
t	=	overall thickness of the shell
U	=	total strain energy of the structure
u, v, w	=	nodal displacements in the local x, y, and z directions, respectively
$\{\boldsymbol{u}\}$	=	global nodal displacement vector
$\{\breve{\boldsymbol{u}}_i\}$	=	vector of the pure nodal displacements for the ith shell element
V	=	volume of a shell element
X	=	set of design variables
x_*	=	shape design variable
$x_*^{(1)}, x_*^{(2)}, \ldots$	=	different definitions for the shape design variable x_*
z	=	distance from the midsurface
Δ	=	control displacement in the nonlinear equilibrium path
$\{\boldsymbol{\varepsilon}\}$	=	vector of the membrane strains, $\{\varepsilon_x \varepsilon_y \gamma_{xy}\}^T$
$\{\boldsymbol{\varepsilon}_o\}$	=	vector of the midsurface membrane strains
η	=	iteration number
$\theta x, \theta y, \theta z$	=	nodal rotations about the local axes x, y and z, respectively
$\{\boldsymbol{\kappa}_o\}$	=	vector of the midsurface curvatures
λ	=	Lagrange multiplier
Π	=	total potential energy
$\tilde{\Pi}$	=	total potential energy associated with the optimal design
ρ	=	material density
$\sum_{x_*}()$	=	sum of all the elements related to shape design variable x_*
υ	=	Poisson's ratio
$()\|_{x_*}$	=	equation valid for all elements affected by the shape design variable x_*

Received 24 January 2006; accepted for publication 9 November 2006.

*Ph.D. Candidate, Department of Mechanical and Industrial Engineering; peyma_kh@encs.concordia.ca. Member AIAA.
†Associate Professor, Department of Mechanical and Industrial Engineering; sedagha@encs.concordia.ca. Member AIAA.
‡Associate Professor, Department of Mechanical and Industrial Engineering; ganesan@encs.concordia.ca.

I. Introduction

THIN-WALLED structures consist of components in the form of plates or shells with small thickness, compared with other dimensions. These structures, which are the most efficient among all of the structural systems, may display nonlinear behavior under applied loads. This kind of nonlinearity, which is due to the large deformations in the structure, is called geometric nonlinearity.

In practical applications, structures have to be optimized to have minimum mass or maximum load capacity. Developing design optimization techniques that efficiently combine the iterative optimization process and iterative nonlinear analysis is a challenging and complex task that has not received appropriate attention. The major problem in the design optimization of nonlinear structures is that the combination of iterative optimization process and iterative nonlinear analysis makes the procedure extremely difficult and, computationally, very expensive. Some designers use the linear analysis instead of iterative nonlinear analysis to increase the efficiency of the optimization process, however, it has been shown [1] that it may lead to infeasible design, which may cause structural failure. Considering this, it is necessary to develop efficient, accurate,

and robust methodologies for design optimization of nonlinear thin-walled structures.

Most of the works on the optimization of structures subject to system stability constraints have been performed on truss structures; these works consider the cross-sectional areas of the members as the design variables. In most of these works, the system stability requirement is posed as a linear buckling analysis [2–9]. Such an analysis is restricted to small deformations in which linear buckling analysis reduces to the solution of a generalized eigenvalue problem. In the case for which the nonlinear behavior results in large changes in the geometry of the structure, this definition of system stability may not be conservative, and a nonlinear buckling analysis should be undertaken.

In most recent works reported in the literature, the optimization algorithms were mainly based on the optimality criterion technique, because of its computational efficiency. For example, the optimality criteria method has been employed to minimize the weight of the truss and beam structures under the stress and displacement constraints [10–13], stability constraint [14,15], or frequency constraint [16]. Modern optimality criterion algorithms would involve the case of satisfying the multiple constraints (scaling) and Karush–Kuhn–Tucker (KKT) [17] condition (resizing) alternatively.

The objective of the present work is to develop a methodology for design optimization of thin-walled structures undergoing large deflections subject to displacement and system stability constraints. In this study, two optimality criteria based on KKT conditions are developed for mass minimization problems. The optimization method considers shape parameters and overall thickness of the structure as the design variables and aims to minimize the total mass of the structure subject to stability or displacement constraint.

II. Problem Definition

The optimization problem is to find a set of design variables to minimize the total mass:

$$M = \rho t \sum_{i=1}^{N} A_i \tag{1}$$

subjected to

$$g = \Pi - \tilde{\Pi} = 0 \tag{2}$$

In this study, the set of design variables consists of shape design variables and overall thickness of the shell. A shape design variable is a parameter that changes the shape of the structure by changing the spatial position of one or several nodal points. It is possible to change the geometry of several elements simultaneously by changing the appropriate shape design variable related to those elements. It is important to note that the change of the shape during optimization should not violate the design constraints or manufacturing requirements. Some studies consider an auxiliary structure to satisfy these requirements during the shape optimization [18,19] . In the present study, change of the shape is performed by shape design variables that do not violate the design constraints and boundary conditions.

Figure 1 shows how a nodal global coordinate can be selected (here, coordinate Z of the point P) as a shape design variable. However, there are other ways for defining a shape design variable. Figure 2 shows how a shape design variable may be defined to control the position of the point P with inclined boundary condition. Assuming that the points P and P' are the positions of a free nodal point moving on line L during the optimization process, shape design variable $x_*^{(1)}$ can be selected as the distance of the free node from a fixed point F. Another way to describe the position of the point is to measure the distance from a fixed point F' on line L, using the shape design variable $x_*^{(2)}$. It is obvious that the number of possible shape design variables that may be defined to describe the position of a node is infinite. However, any manufacturing requirement, such as a straight edge remaining straight or portions of the boundary

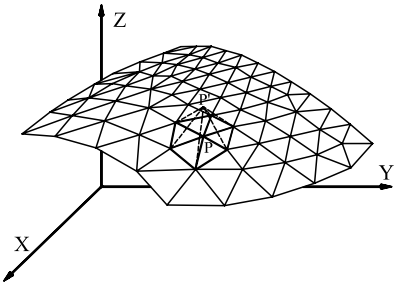

Fig. 1 Considering the nodal coordinate as the shape design variable.

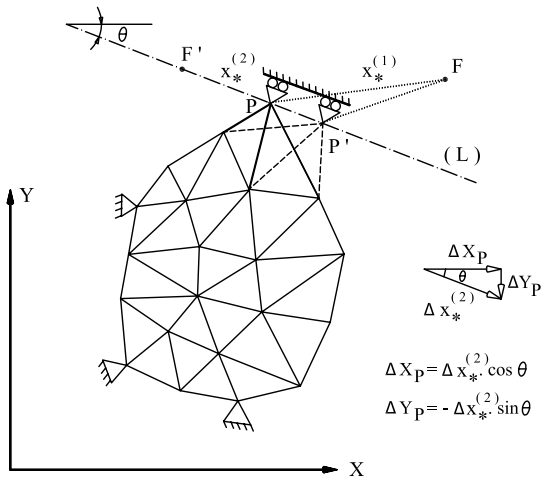

Fig. 2 Definition of the shape design variable.

remaining unchanged, should be considered when defining a shape design variable. It should be noted that in this example, a shape design variable changes both coordinates X and Y simultaneously, because point P is moving on line L, due to its inclined boundary condition.

III. Optimization Criteria

In this section, an optimization criteria is found for mass minimization problem, using an approach similar to the one used by Khot and Kamat [14], and Sedaghati and Tabarrok [15] for mass minimization of truss structures. To simplify the presentation, and without loss of generality, it will be considered that the shape of the structure is described by only one shape design variable and overall thickness. The total potential energy of the structure may be expressed as

$$\Pi = \sum_{i=1}^{N} e_i - \{\boldsymbol{u}\}^T\{\boldsymbol{R}\} = U - \{\boldsymbol{u}\}^T\{\boldsymbol{R}\} \tag{3}$$

where the strain energy of the ith shell element may be written as

$$e_i = \frac{1}{2}\{\breve{\boldsymbol{u}}_i\}^T[k_i]\{\breve{\boldsymbol{u}}_i\} \tag{4}$$

where $\{\breve{\boldsymbol{u}}_i\}$ displacements are after removing the rigid body motions, due to large deflections. It should be mentioned that pure displacements may also be generally written as a function of $\{\boldsymbol{u}\}$. From the principal of stationary total potential energy, we have

$$\frac{\partial \Pi}{\partial \{\boldsymbol{u}\}} = \frac{\partial U}{\partial \{\boldsymbol{u}\}} - \{\boldsymbol{R}\} = \{0\} \tag{5}$$

Using Eqs. (1) and (2), the Lagrangian can be defined as

$$\mathcal{L} = \rho t \sum_{i=1}^{N} A_i - \lambda(\Pi - \tilde{\Pi}) \tag{6}$$

The KKT conditions [17] for minimization of $\mathcal{L}$ with respect to x_* and t become

$$\frac{\partial \mathcal{L}}{\partial x_*} = 0 \tag{7}$$

$$\frac{\partial \mathcal{L}}{\partial t} = 0 \tag{8}$$

$$\Pi - \tilde{\Pi} = 0 \tag{9}$$

It is obvious that in cases with several shape design variables, Eq. (7) is valid for each x_* . From Eqs. (3), (6), and (7), we have

$$\rho t\left(\sum_{x_*} \frac{\partial A_i}{\partial x_*}\right) - \lambda\left(\sum_{x_*} \frac{\partial e_i}{\partial x_*} + \sum_{j=1}^{m} \frac{\partial \Pi}{\partial u_j}\frac{\partial u_j}{\partial x_*}\right) = 0 \tag{10}$$

Considering Eq. (5), the term $\partial\Pi/\partial u_j$ vanishes and Eq. (10) may be written as

$$\rho t\left(\sum_{x_*} \frac{\partial A_i}{\partial x_*}\right) - \lambda\left(\sum_{x_*} \frac{\partial e_i}{\partial x_*}\right) = 0 \tag{11}$$

or

$$\rho t\left(\sum_{x_*} \frac{\partial A_i}{\partial x_*}\right) - \lambda\left(\sum_{x_*} \frac{\partial e_i}{\partial A_i}\frac{\partial A_i}{\partial x_*}\right) = 0 \tag{12}$$

Because the strain energy of a flat shell element is in proportion to the element area, $\partial e_i/\partial A_i = e_i/A_i$. Thus,

$$\sum_{x_*}\left(\rho t - \lambda\frac{e_i}{A_i}\right)\left(\frac{\partial A_i}{\partial x_*}\right) = 0 \tag{13}$$

or

$$\sum_{x_*}\left(1 - \lambda\frac{e_i}{\rho t A_i}\right)\left(\frac{\partial A_i}{\partial x_*}\right) = 0 \tag{14}$$

Defining the strain energy density as $\hat{e}_i = e_i/(\rho t A_i)$, we have

$$\sum_{x_*}(1 - \lambda\hat{e}_i)\left(\frac{\partial A_i}{\partial x_*}\right) = 0 \tag{15}$$

As discussed before, there are infinite possibilities to define a shape design variable, because it can be defined as the distance from various fixed points. The terms $(1 - \lambda\hat{e}_i)$ in Eq. (15) are independent of the definition of x_*, and as a result, these terms do not change if x_* is defined differently. However, the terms $(\partial A_i/\partial x_*)$ depend on the definition of x_* and change if x_* is defined in another way. Considering that Eq. (15) is valid at the optimum point, independent of how x_* is defined, we have

$$\begin{cases} \sum_{x_*}(1 - \lambda\hat{e}_i)\left(\frac{\partial A_i}{\partial x_*^{(1)}}\right) = 0 \\ \sum_{x_*}(1 - \lambda\hat{e}_i)\left(\frac{\partial A_i}{\partial x_*^{(2)}}\right) = 0 \\ \cdots \end{cases} \tag{16}$$

Equation (16) is a set of simultaneous homogeneous equations, with $\partial A_i/\partial x_*^{(1)}$, $\partial A_i/\partial x_*^{(2)}, \ldots$ as the coefficients and $(1 - \lambda\hat{e}_i)$ as the unknowns. This set always has the following trivial solution:

$$(1 - \lambda\hat{e}_i) = 0|_{x_*} \Rightarrow (1 = \lambda\hat{e}_i)|_{x_*} \tag{17}$$

This uniform strain energy density criterion equation states that in an optimum structure, the strain energy density of all elements affected by the design variables are the same. Applying similar steps for Eq. (8), we have

$$\rho\left(\sum_{i=1}^{N} A_i\right) - \lambda\left(\sum_{i=1}^{N} \frac{\partial e_i}{\partial t}\right) = 0 \tag{18}$$

Considering Eq. (17) and substituting $\lambda = 1/\hat{e}_i = \rho t A_i/e_i$ into Eq. (18), we may have the following criterion for all possible optimum solutions:

$$\sum_{i=1}^{N}\left(\rho A_i - \frac{\rho t A_i}{e_i}\cdot\frac{\partial e_i}{\partial t}\right) = 0 \tag{19}$$

or

$$\sum_{i=1}^{N} \rho A_i\left[1 - \left(\frac{\partial e_i}{\partial t}\right)\Big/\left(\frac{e_i}{t}\right)\right] = 0 \tag{20}$$

In the case of pure membrane behavior, strain energy is provided by only the membrane stiffness, thus e_i is in proportion to t and $(\partial e_i/\partial t)$ is equal to (e_i/t). In any other case, $(\partial e_i/\partial t)$ is always greater than (e_i/t), because of the t^2 and t^3 terms associated with the membrane-bending coupling and pure bending behavior, respectively. So in the general case, $(\partial e_i/\partial t)$ is always equal to or greater than (e_i/t), and all the terms in the sum in Eq. (20) are negative or zero. Thus, the only possible solution for Eq. (20) is

$$\frac{\partial e_i}{\partial t} = \frac{e_i}{t} \tag{21}$$

which states that at the optimum point, all the strain energy is provided by the membrane mode. In other words,

$$\frac{e_{ib}}{e_i} \to 0 \tag{22}$$

This relation may also be extended to the whole structure:

$$\frac{\text{total bending strain energy}}{\text{total strain energy}} = \frac{\Sigma e_{ib}}{\Sigma e_i} \to 0 \tag{23}$$

This bending energy ratio criterion relation states that among all optimum designs with different thicknesses, the one that has the least bending energy ratio has the minimum mass. Equations (17) and (23) are called optimality criteria and should be satisfied to minimize the total mass of a shell structure.

IV. Recurrence Relation

To satisfy the uniform strain energy density criterion, an iterative scheme is used. First, Eq. (17) is rewritten in the form of $\rho t A_i = \lambda e_i$ and then it is applied to all elements connected to x_*:

$$\begin{aligned} \rho t A_1 &= \lambda e_1 \\ \rho t A_2 &= \lambda e_2 \\ &\cdots \\ \rho t A_k &= \lambda e_k \end{aligned} \tag{24}$$

Summing both sides, we have

$$\rho t\sum_{j=1}^{k} A_j = \lambda\sum_{j=1}^{k} e_j \tag{25}$$

or

$$1 = \lambda\frac{\sum_{j=1}^{k} e_j}{\rho t\sum_{j=1}^{k} A_j} \tag{26}$$

The recurrence relation may be written by multiplying both sides of this equation by x_* and taking the rth root:

$$(x_*)_{\eta+1} = (x_*)_\eta \cdot \left(\lambda\frac{\sum_{j=1}^{k} e_j}{\rho t\sum_{j=1}^{k} A_j}\right)^{1/r} \tag{27}$$

where $\eta + 1$ and η are the iteration numbers, and r can be changed by assigning an appropriate value.

The value of the Lagrange multiplier at the optimal design is found from Eq. (17) by minimizing the sum of the squares of the residuals at iteration η:

$$Res_\eta = \sum_{i=1}^{N_e} (1 - \lambda \hat{e}_i)^2 \tag{28}$$

Thus, the Lagrange multiplier can be obtained as

$$\lambda = \frac{\sum_{i=1}^{N_e} \hat{e}_i}{\sum_{i=1}^{N_e} \hat{e}_i^2} \tag{29}$$

Substituting Eq. (29) into Eq. (27), we finally obtain

$$(x_*)_{\eta+1} = (x_*)_\eta \cdot \left(\frac{\sum_{i=1}^{N_e} \hat{e}_i}{\sum_{i=1}^{N_e} \hat{e}_i^2} \cdot \frac{\sum_{j=1}^{k} e_j}{\rho t \sum_{j=1}^{k} A_j} \right)^{1/r} \tag{30}$$

This relation is used to iteratively modify the shape and approach to the optimal design. The other optimality criterion, Eq. (23), is used to guarantee that change of the thickness to scale the design (which is explained in the next section) is in the proper direction toward the optimal design. Obviously, if the overall thickness of the structure is not considered as a design variable, this optimality criterion is relaxed and scaling is done by changing shape design variables.

V. Solution Methodology

The shell element used in this study [20] is a thin triangular element, shown in Fig. 3, with 18 degrees of freedom, 3 rotations, and 3 displacements per node. The element nodal displacement vector can be described as

$$\{\boldsymbol{d}\} = \{\, u_1 \quad v_1 \quad w_1 \quad \theta x_1 \quad \theta y_1 \quad \theta z_1 \quad u_2 \quad v_2 \quad w_2 \quad \dots \quad \theta z_3 \,\}^T \tag{31}$$

This element is a combination of optimal membrane triangle (OPT) [21] and discrete Kirchhoff triangle [22] elements. The OPT membrane element is called optimal because, for any arbitrary aspect ratio, its strain energy for in-plane pure bending is exact.

The strain energy of the ith element is expressed as

$$e_i = \frac{1}{2} \int_V \{\boldsymbol{\varepsilon}\}^T [E] \{\boldsymbol{\varepsilon}\} \, \mathrm{d}V \tag{32}$$

Relating the strains to the midsurface strains and midsurface curvatures, the strain energy is

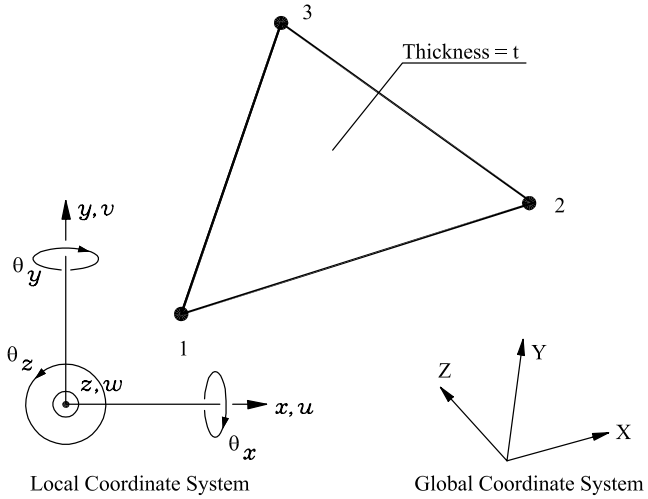

Fig. 3 Geometry of the triangular shell element.

$$e_i = \frac{1}{2} \int_V \{\boldsymbol{\varepsilon}_o + z\boldsymbol{\kappa}_o\}^T [E] \{\boldsymbol{\varepsilon}_o + z\boldsymbol{\kappa}_o\} \, \mathrm{d}V \tag{33}$$

or

$$e_i = \frac{1}{2} \int_A (\{\boldsymbol{\varepsilon}_o\}^T [A^e] \{\boldsymbol{\varepsilon}_o\} + \{\boldsymbol{\varepsilon}_o\}^T [B^e] \{\boldsymbol{\kappa}_o\} + \{\boldsymbol{\kappa}_o\}^T [B^e] \{\boldsymbol{\varepsilon}_o\} + \{\boldsymbol{\kappa}_o\}^T [D^e] \{\boldsymbol{\kappa}_o\}) \, \mathrm{d}A \tag{34}$$

where $[A^e]$, $[B^e]$, and $[D^e]$, in the case of laminated composite plates and shells, can be written as [23]

$$A_{ij}^e = \sum_{k=1}^{n} (z_k - z_{k-1}) E_{ij}^k \qquad B_{ij}^e = \sum_{k=1}^{n} \frac{1}{2} \left(z_k^2 - z_{k-1}^2 \right) E_{ij}^k$$
$$D_{ij}^e = \sum_{k=1}^{n} \frac{1}{3} \left(z_k^3 - z_{k-1}^3 \right) E_{ij}^k \qquad (n = number\ of\ layers) \tag{35}$$

In the case of isotropic material with Poisson's ratio and Young's modulus,

$$E = \frac{E_\circ}{1 - \upsilon^2} \begin{bmatrix} 1 & \upsilon & 0 \\ \upsilon & 1 & 0 \\ 0 & 0 & \frac{1-\upsilon}{2} \end{bmatrix}, \qquad [A^e] = t[E]$$
$$[D^e] = \frac{t^3}{12} [E], \qquad [B^e] = [0]_{3\times 3} \tag{36}$$

To analyze the structures with geometric nonlinearity, a corotational approach is used [20,24]. In this approach, the total motion of an element is decomposed into a rigid body motion and a pure deformation. The contribution of the rigid body motion to the total deformation of the element is removed before performing the element computations. This will allow an upgrade of the structural elements to treat problems with large rotations and small strains. This is the case with many thin-walled plate and shell structures undergoing large deformations.

It should be mentioned that some doubts have recently been raised about the mathematical convergence of facet elements [25]. In particular, when refining the mesh, finite element solutions are expected to converge to the exact solution of a well-defined mathematical model. However, some numerical experiments have shown that facet shell elements may not exactly converge when the mesh is refined, although their results are very close to the reference values [25]. It is believed that the best shell elements are formulated using 3-D continuum mechanics incorporating shell theory assumptions. However, facet elements are used in this study, because the formulation of a corotational approach using curved elements is extremely difficult to perform and it is not even well developed. It may be noted that for the case of nonlinear behavior with small pure deformations, the corotational method is the most effective approach, because it takes advantage of existing small-strain elements during the analysis [26].

Figure 4 shows two cases of nonlinear response with limit loads. Figure 4a is called snap-through behavior, which is one of the most frequent forms of nonlinear response of shallow structures. Figure 4b shows another case in which the structure has no post-buckling strength. In both cases, the limit point is identified as the point at which the tangent stiffness matrix becomes singular. The load level at the limit point is selected as the constraint for optimization against system stability.

In practical cases, the tangent stiffness matrix rarely becomes exactly singular; thus, in this study, an alternative method is used to find the limit load of the nonlinear path. Because the arc-length method [27] is capable of tracing the post-buckling path, one can use this method to follow the equilibrium path beyond the limit point. As shown in Fig. 4c, analysis is stopped when the load level at a newly converged point of the path (point 3) becomes less than that of the previous converged point (point 2). Using the values corresponding to the three last points 1, 2, and 3, it is possible to perform a quadratic fit to the load-displacement curve near the limit point and find F_{cr}.

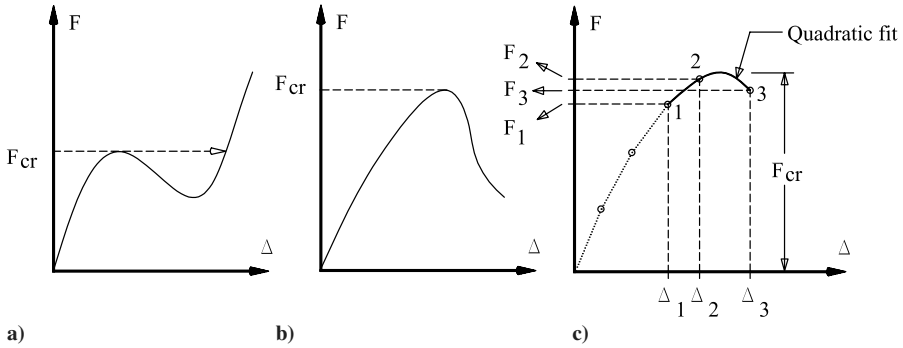

Fig. 4 Two forms of the nonlinear response curve with limit load.

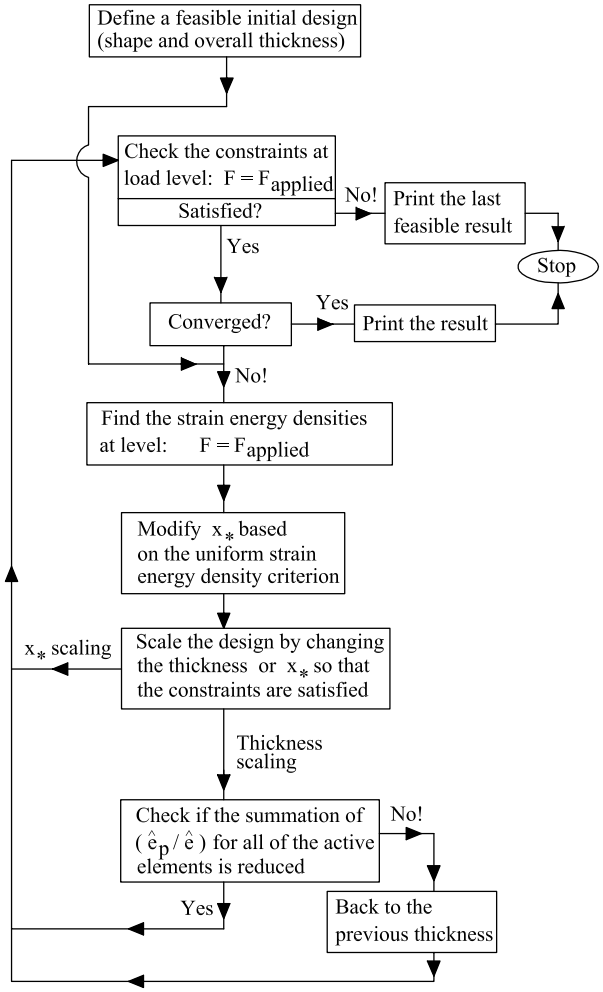

Fig. 5 Flowchart of the proposed optimization algorithm.

The peak load determined through this procedure was found to be very accurate.

Figure 5 shows the optimization algorithm based on the proposed optimality criteria. In this study, the optimization constraint is either the system stability or the nodal displacement. In the case for which the system stability is the optimization constraint, the solution after each iteration should be scaled so that the limit load of the structure is equal to or greater than the applied load. The same procedure is done for the case of displacement constraint to limit the nodal displacement to a maximum allowable value. It is possible to scale the design by changing the general thickness of the shell. Obviously, if the limit load is greater than the applied load, the thickness should be reduced and vice versa. As for displacement constraint, if the maximum displacement is greater than the allowable displacement, the thickness should be increased and vice versa.

It should be noted that the strain energy is not a linear function of the thickness, and as a result, scaling the thickness of the shell by a scale factor does not have the effect of scaling the limit load by the same scale factor. In other words, by changing the thickness of the shell, the displacement pattern also changes, and a simple proportional reduction or increase of the thickness would not lead to the desired critical load. Selecting the new thickness is usually done through an iterative process. However, this process is not highly iterative, because the new thickness is usually selected among a set of available thicknesses, and this process converges after a few iterations.

Considering the thickness of the shell as one of the design variables and scaling the solution by changing the thickness does not always lead to a suitable design. One example is a thin cantilever plate subjected to an end vertical load. By trying to scale the design to satisfy the displacement constraint, the solution converges to a narrow, but thick, structure, which is not necessarily in agreement with the assumed bending element. In this case, a better result is found by relaxing the second optimality criterion, Eq. (23), and using just the shape design variables to scale the design. This technique is used in examples 2 and 3 of the following section.

Although Eq. (30) guaranties that the design iteratively approaches the optimal design, true optimality is not always possible. This means that in the final design, the strain energy density distribution may not be completely uniform.

VI. Numerical Results

To demonstrate the efficiency and accuracy of the proposed design optimization methodology, three illustrative examples are presented. Stability and displacement constraints are considered in the first and second examples, respectively. The third example is again an optimization problem with stability constraint, in which the accuracy of the proposed algorithm is compared with that of the sequential quadratic programming (SQP) gradient-based method. Regarding the sensitivity analysis, an analytical method has been presented in [28] that is independent of the element type and is valid for shape and size design variables. However, because the main idea in the third example is to only evaluate the accuracy of the proposed method by comparing its result with that of the gradient-based methods, the finite difference method (FDM) is used as an alternative approach for sensitivity analysis in the SQP method:

$$\frac{\mathrm{d}f}{\mathrm{d}x} = \frac{f(x+\Delta x) - f(x)}{\Delta x} \tag{37}$$

The accuracy of the FDM is dependent on the perturbation size Δx. A relative perturbation between 10^{-5} and 10^{-8} generally leads to results with sufficient accuracy for engineering applications.

A. Example 1: Shallow Spherical Shell Under Transverse Load

Figure 6 shows a shallow spherical shell subjected to an 8000-N downward load at the top. The optimization problem is to minimize the total mass of the shell subject to stability constraint. This means that F_{cr} in the optimum design should be equal or very close to (but more than) 8000 N. The shell is modeled with 144 triangular

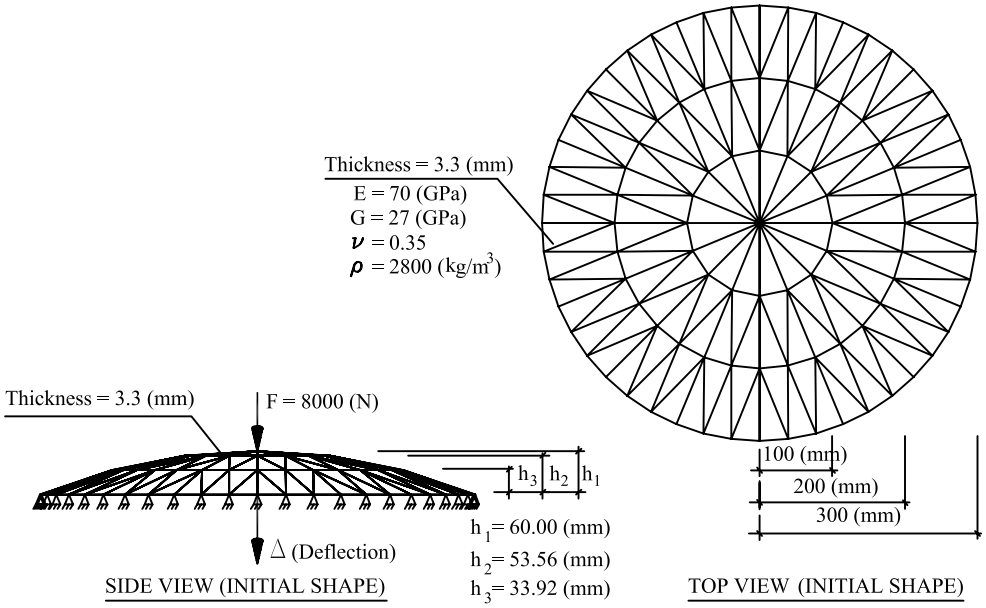

Fig. 6 Shallow spherical shell subject to transverse load.

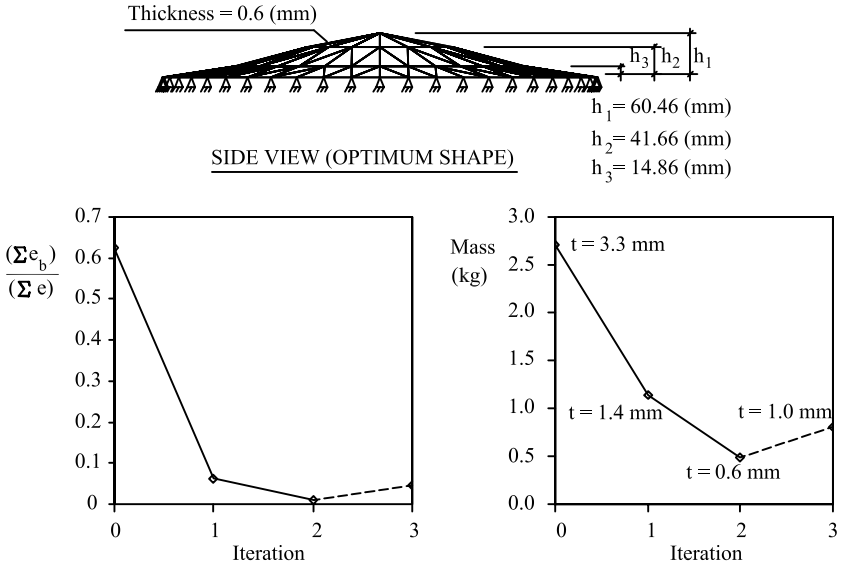

Fig. 7 Optimum shape and variation of the mass and bending energy ratio for the dome shell (thickness scaling).

elements and, due to symmetry, only a quarter of the shell is analyzed. The shape design variables are considered to be h_1, h_2, and h_3, with initial values of 60.00, 53.56, and 33.92 mm, respectively. The initial value of $t = 3.3$ mm is considered for the overall thickness of the shell. The initial total mass is equal to $M = 2.7110$ kg, assuming the mass density to be equal to 2800 kg/m^3. The optimization procedure starts by changing the nodal positions in the vertical direction and considering the step-size parameter $r = 10$. Three regions have been considered ($h > h_2$, $h_2 > h > h_3$, and $h_3 > h$), and to eliminate the effect of mesh configuration, the average value of the strain energy density in each region has been considered in the optimization process.

Figure 7 shows the results of optimization (optimum shape, bending energy ratio, and mass iteration histories) based on the proposed algorithm. In this analysis, the design is scaled at each iteration by changing the overall thickness of the shell. The minimum change in the thickness is assumed to be equal to 0.1 mm. In the third iteration, the bending energy ratio increases, which means that the change in the thickness due to the design scaling is not in the proper direction toward the optimal design. Based on the algorithm, the analysis should be continued with the previous thickness, but it is not possible, because of the stability constraint. Thus, the analysis terminates and the minimum mass $M = 0.4844$ kg is achieved in the second iteration.

As an example of the design variable linking, we may consider the case for which the overall shape of the shell remains spherical during the shape optimization. In this case, only h_1 is the shape design variable, and h_2 and h_3 should be linked to h_1. Linking the design variables may be done in different ways, however, it is always preferred to avoid high aspect ratio elements during optimization. For example, the following relation ensures that all elements are of the same relative size and aspect ratio during the shape optimization, as shown in Fig. 8:

$$h_2 = R(\cos\theta - \cos 3\theta), \qquad h_3 = R(\cos 2\theta - \cos 3\theta) \tag{38}$$

in which $R = (300^2 + h_1^2)/2h_1$ and $\theta = \frac{1}{3}\sin^{-1}(300/R)$. In this case, the design variable h_1 controls the position of all free nodal points, and optimum solution is obtained when the strain energy densities become uniform all over the shell, using the same methodology.

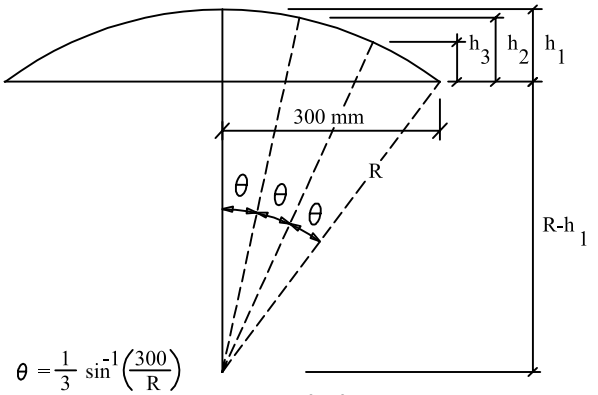

Fig. 8 Linking the design variables for the spherical dome shell.

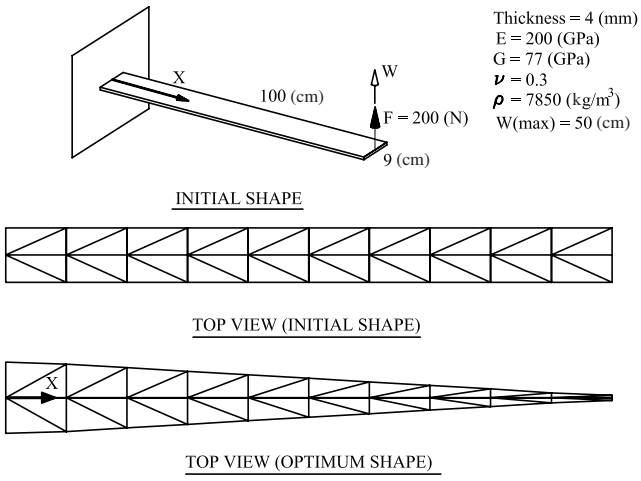

Fig. 9 Cantilever plate with end load.

B. Example 2: Cantilever Plate with End Load

In this example, the proposed algorithm is used to optimize a plate with displacement constraint. A cantilever plate with end load $F = 200$ N is shown in Fig. 9, and the objective is to minimize the mass of the plate subject to a displacement constraint $W < 50$ cm at the tip.

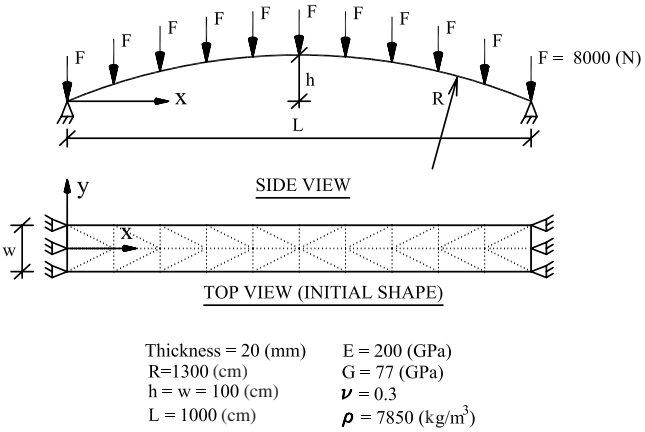

Fig. 11 Shallow arch under downward loads.

The initial dimensions of 9×100 cm and thickness of $t = 4$ mm are considered for the plate. The initial total mass of the plate, considering a mass density of $\rho = 7850$ kg/m^3, is $M = 2.8260$ kg. The plate is modeled with 40 triangular elements and, due to symmetry, only half of the plate is analyzed. The width of the plate at each station is considered as the shape design variable.

In this example, design scaling by changing the thickness will result in a narrow, but thick, plate, which is not desirable. To minimize the mass and keep the same thickness, design scaling is done by multiplying the width of the plate at every point by a scaling factor. Because the design scaling is not done by changing the thickness, it is not required to check if the bending energy ratio decreases. Similar to the previous example, the step-size parameter is considered as $r = 10$.

Figure 10 shows the optimum shape and variation of $\rho\hat{e}_i$ over the length of the cantilever plate before and after optimization. It can be seen that the total mass decreases to $M = 2.0116$ kg, whereas the strain energy density approaches the uniform distribution.

C. Example 3: Shallow Arch Under Downward Loads

Figure 11 shows a shallow shell with thickness $t = 20$ mm subjected to 11 concentrated vertical loads, each one equal to $F = 8000$ N. The optimization problem is to find the best shape (by varying the width of the arch, and without any change in the thickness) to have minimum mass subject to the stability constraint. The plate is modeled with 40 triangular elements and, due to symmetry, only a quarter of the plate is analyzed. The step-size parameter $r = 2$ is considered in analysis. The width of the shell at each station with an initial value of $W = 100$ cm is considered as the

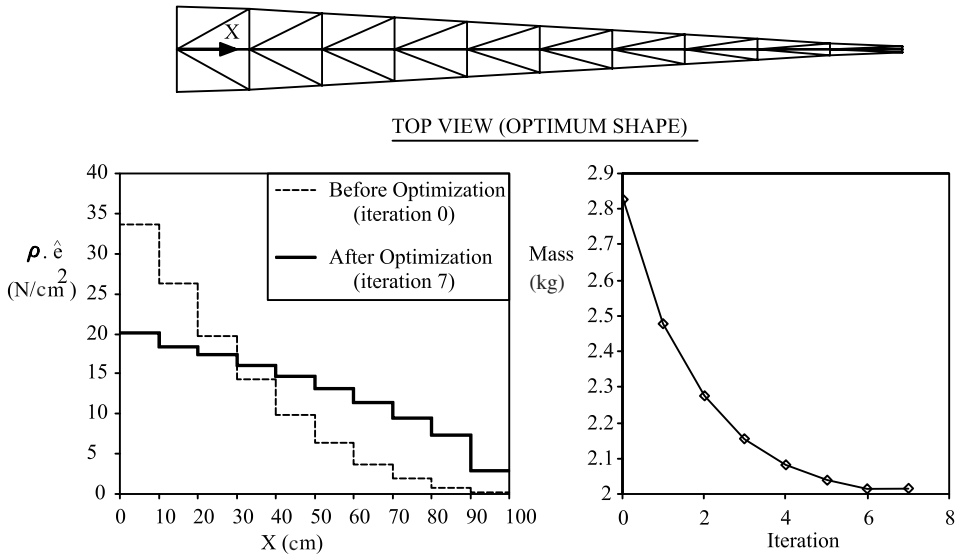

Fig. 10 Optimum shape and variation of the mass and energy density for the cantilever plate.

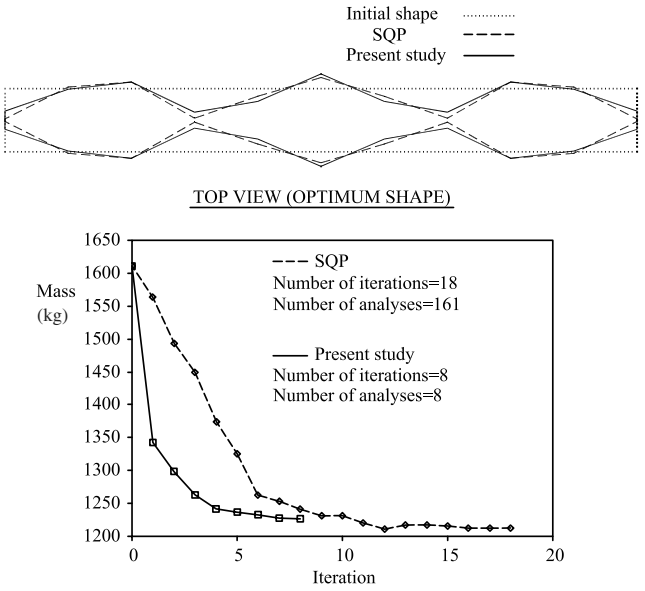

Fig. 12 Optimum shapes and variation of the mass for the shallow shell (present study vs the SQP method).

shape design variable. Similar to the previous example design, scaling is performed by changing the width of the shell at each point. As mentioned before, because the thickness is kept constant during the optimization, the second criterion (bending energy ratio) is relaxed.

Figure 12 shows the result obtained by this study compared with the one obtained by the SQP method. Starting with the initial mass $M = 1611.12$ kg, the minimum mass obtained by the proposed method after eight iterations and performing eight nonlinear analyses is $M = 1226.30$ kg. Analysis by the SQP method leads to a smaller mass equal to $M = 1213.10$ kg, but it needs 18 iterations and 161 nonlinear analyses. It may be seen that by using the proposed design optimization methodology, one can efficiently obtain the optimum solution with an acceptable accuracy without any need to perform the time-consuming task of sensitivity analysis. It should be mentioned that in this example, scaling the width of the shell by a scale factor has the effect of scaling the limit load by the same scale factor, which makes the scaling process easy to perform without any new iteration. Even in the case of scaling by thickness, in which the load-displacement pattern changes after each scaling, the authors' experience shows that the total number of analyses is much less than that necessary in the SQP gradient-based method.

VII. Conclusions

A new methodology for optimization of thin plate and shell structures has been developed. Two optimality criteria have been proposed and combined with a nonlinear analysis program. The method tries to change the shape of the structure so that the strain energy densities in all elements affected by the change in the shape of the structure have the same value. It has been shown that this method converges to an optimal shape and requires fewer analyses than the standard gradient-based methods of optimization. It is concluded that the complex task of shape optimization in nonlinear structures can be performed efficiently by the proposed methodology.

The proposed method seems to be suitable for cases in which the shape of the structure can be defined by a few number of design variables, and the nodal positions in the finite element mesh are linked to the design variables by a suitable relation. It should be mentioned that structural optimization techniques based on optimality criteria method may suffer convergence difficulties and other numerical instabilities when they are applied to the optimum design of large structures. This is why stochastic search techniques such as genetic algorithm and simulated annealing have recently found wide application in structural optimization. Further studies on this aspect will be conducted by the present authors to determine the performance of the proposed algorithm in the design of large scale structures.

References

[1] Lee, S. J., and Hintonz, E., "Dangers Inherited in Shells Optimized with Linear Assumptions," *Computers and Structures*, Vol. 78, Nos. 1–3, 2000, pp. 473–486.

[2] Kiusalaas, J., "Optimal Design of Structures with Buckling Constraints," *International Journal of Solids and Structures*, Vol. 9, No. 7, 1973, pp. 863–878.

[3] Khot, N. S., Venkayya, V. B., and Berke, L., "Optimum Structural Design with Stability Constraints," *International Journal for Numerical Methods in Engineering*, Vol. 10, No. 5, 1976, pp. 1097–1114.

[4] Khot, N. S., "Optimal Design of a Structure for System Stability for a Specified Eigenvalue Distribution," *International Symposium on Optimum Structural Design*, Univ. of Arizona, Tucson, AZ, 1981.

[5] Khot, N. S., "Nonlinear Analysis of Optimized Structure with Constraints on System Stability," *AIAA Journal*, Vol. 21, No. 8, 1983, pp. 1181–1186.

[6] Levy, R., and Perng, H. S., "Optimization for Nonlinear Stability," *Computers and Structures*, Vol. 30, No. 3, 1988, pp. 529–535.

[7] Szyskowski, W., Watson, L. G., and Fietkiewicz, B., "Bimodal Optimization of Frames for Maximum Stability," *Computers and Structures*, Vol. 32, No. 5, 1989, pp. 1093–1104.

[8] Canfield, R. A., "Design of Frames Against Buckling Using a Rayleigh Quotient Approximation," *AIAA Journal*, Vol. 31, No. 6, 1993, pp. 1144–1149.

[9] Levy, R., "Optimal Design of Trusses for Overall Stability," *Computers and Structures*, Vol. 53, No. 5, 1994, pp. 1133–1138.

[10] Saka, M. P., "Optimum Design of Space Trusses with Buckling Constraints," *Proceedings of the Third International Conference on Space Structures*, Univ. of Surrey, Guildford, England, U.K., 1984.

[11] Saka, M. P., and Ulker, M., "Optimum Design of Geometrically Nonlinear Space Trusses," *Computers and Structures*, Vol. 42, No. 3, 1992, pp. 289–299.

[12] Khan, M. R., "Optimality Criterion Techniques Applied to Frames Having General Cross-Sectional Relationships," *AIAA Journal*, Vol. 22, No. 5, 1984, pp. 669–676.

[13] Khan, M. R., Willmert, K. D., and Thornton, W. A., "A New Optimality Criterion Method for Large Scale Structures," *Proceedings of the AIAA/ASME 19th Structures, Structural Dynamics, and Materials Conference*, AIAA, New York, 1978, pp. 47–58.

[14] Khot, N. S., and Kamat, M. P., "Minimum Weight Design of Truss Structures with Geometric Nonlinear Behavior," *AIAA Journal*, Vol. 23, No. 1, 1985, pp. 139–144.

[15] Sedaghati, R., and Tabarrok, B., "Optimum Design of Truss Structures Undergoing Large Deflections Subject to a System Stability Constraint," *International Journal for Numerical Methods in Engineering*, Vol. 48, No. 3, 2000, pp. 421–434.

[16] Grandhi, R. V., and Venkayya, V. B., "Structural Optimization with Frequency Constraints," *AIAA Journal*, Vol. 26, No. 7, 1988, pp. 858–866.

[17] Arora, J. S., *Introduction to Optimum Design*, McGraw–Hill, New York, 1989.

[18] Rajan, S. D., and Belegundu, A. D., "Shape Optimal Design Using Fictitious Loads," *AIAA Journal*, Vol. 27, No. 1, 1989, pp. 102–107.

[19] Belegundu, A. D., and Rajan, S. D., "A Shape Optimization Approach Based on Natural Design Variables And Shape Functions," *Computer Methods in Applied Mechanics and Engineering*, Vol. 66, No. 1, 1988, pp. 87–106.

[20] Khosravi, P., Ganesan, R., and Sedaghati, R., "Corotational Nonlinear Analysis of Thin Plates and Shells Using a New Shell Element," *International Journal for Numerical Methods in Engineering* (to be published).

[21] Felippa, C. A., "A Study of Optimal Membrane Triangles with Drilling Freedoms," *Computer Methods in Applied Mechanics and Engineering*, Vol. 192, No. 16, 2003, pp. 2125–2168.

[22] Batoz, J. L., Bathe, K. J., and Ho, L. W., "A Study of Three-Node Triangular Plate Bending Elements," *International Journal for Numerical Methods in Engineering*, Vol. 15, No. 12, 1980, pp. 1771–1812.

[23] Berthelot, J. M., *Composite Materials: Mechanical Behaviour and Structural Analysis*, Springer, New York, 1999.

[24] Rankin, C. C., and Brogan, F. A., "An Element Independent Corotational Procedure for the Treatment of Large Rotations," *Journal*

of Pressure Vessel Technology, Vol. 108, May 1986, pp. 165–174.

[25] Chapelle, D., *The Finite Element Analysis of Shells: Fundamentals*, Springer, New York, 2003.

[26] Felippa, C. A., "A Systematic Approach to the Element-Independent Corotational Dynamics of Finite Elements," *IASS-IACM 2000: Fourth International Colloquium on Computation of Shell and Spatial Structures* [CD-ROM], Inst. of Structural Analysis and Seismic Research, Athens, Greece, 2000.

[27] Crisfield, M. A., "A Fast Incremental/Iterative Solution Procedure that Handles Snap-Through," *Computers and Structures*, Vol. 13, Nos. 1–3, June 1981, pp. 55–62.

[28] Parente, E., and Vaz, L. E., "On Evaluation of Shape Sensitivities of Non-Linear Critical Loads," *International Journal for Numerical Methods in Engineering*, Vol. 56, No. 6, 2003, pp. 809–846.

A. Messac
Associate Editor